IEEE Xplore® Document Notice

Please Note:

Figure 1 has been removed from view due to copyright concerns.

We regret any inconvenience.

Key Technologies for Integration of Multitype Renewable Energy Sources—Research on Multi-Timeframe Robust Scheduling/Dispatch

Haoyong Chen, *Senior Member, IEEE*, Peizheng Xuan, Yongchao Wang, Ke Tan, and Xiaoming Jin

***Abstract*—Large-scale integration of multitype renewable energy (RE) sources (intermittent energy sources) has become an important feature in smart grid development all over the world. It is internationally recognized that the island (or weak-tie connected) power grids are the best platforms for intermittent energy integration test and demonstration because of their abundant RE resources, scarcity of conventional energy, and technical difficulty with accommodation of intermittent energy. The ongoing research on Hainan (the second biggest island in China) power grid will achieve a comprehensive breakthrough in power grid planning, analysis, scheduling, operation, relay protection, security control, disaster prevention, and other key areas in multitype RE source integration. To be specific, this paper focuses on the key part of the research project—optimal scheduling and complementary operation and a new framework of multitime-frame robust scheduling/dispatch system is first proposed, which is different from most other robust approaches and lays special emphasis on the engineering characteristics of power system operation. Simulation results based on the real data of Hainan power grid show that the approach presented is effective and will be put into online operation in the near future.**

***Index Terms*—Intermittent energy source, island power grid, optimal scheduling/dispatch, robustness, smart grids.**

NOMENCLATURE

Variables

n, m, r, d, c, j, y	Index of coal units/ hydro units/ natural gas units/ nuclear units/ pumped-storage units/ wind farm/ photovoltaic plant.
g	Index of conventional units.
g'	Index of renewable energy (RE) units.
t	Index of dispatch period.
l	Index of lines.
$P_g(n,t), P_v(m,t), P_q(r,t), P_e(d,t), P_x(c,t), P_w(j,t), P_f(y,t)$	Generation of coal unit n, hydro unit m, natural gas unit r, nuclear units d, pumped-storage units c, wind farm j and photovoltaic plant y at period t, respectively.
$P(g,\ t)$	Generation of conventional unit g at period t.
$P(g',\ t)$	Generation of RE unit g' at period t.
$Q(m,\ t)$	Cumulative generating flow of hydro unit m by period t.
$\Delta P_x(c,t)$	Cumulative generation of pumped-storage units c by period t.
$P_{(0)}(g,t)$	Generation of conventional unit g at period t in day-ahead scheduling.
k	Index of the number of rolling dispatch.
$P(g,t)_{(k)}$	Generation of conventional unit g at period t in kth ($k>1$) rolling dispatch horizon.
$\delta(l,t)$	Power flow margin index in l at period t.
$\delta_{\text{sum}}(l)$	Sum of power flow margin of all periods in l.
$P_L(l,t)$	Power flow in l at period t.

Constants

N, M, R, D, C, J, Y	Total number of coal units/ hydro units/ natural gas units/ nuclear units/ pumped-storage units/ wind farms/ photovoltaic plants.
Ns	Total number of error scenarios.
T	Number of dispatch periods in a scheduling/dispatch horizon.
L	Total number of lines.
τ	Length of a dispatch period (in minute).
τ_c	Allowed time of power adjustment between different scenarios.
$P_D(t)$	Load at period t.
γ	Spinning reserve rate.
$P_{\min}(g)$	Minimum output of conventional unit g.
$P_{\max}(g)$	Maximum output of conventional unit g.

Manuscript received February 28, 2014; revised July 22, 2014 and November 1, 2014; accepted December 23, 2014. Date of publication January 26, 2015; date of current version December 19, 2015. This work was supported in part by the China National Funds for Excellent Young Scientists under Grant 51322702, and in part by the National Natural Science Foundation of China under Grant 51177049. Paper no. TSG-00177-2014.

H. Chen is with the School of Electric Power, South China University of Technology, Guangzhou 510641, China, and also with the Asia-Pacific Research Institute of Smart Grid and Renewable Energy, Hong Kong (e-mail: eehychen@scut.edu.cn).

P. Xuan, Y. Wang, and K. Tan are with the School of Electric Power, South China University of Technology, Guangzhou 510641, China.

X. Jin is with the Electric Power Research Institute of China Southern Power Grid, Guangzhou 510080, China.

Color versions of one or more of the figures in this paper are available online at http://ieeexplore.ieee.org.

Digital Object Identifier 10.1109/TSG.2015.2388756

$R_u(g)$, $R_d(g)$	Ramp-up/ramp-down rate of conventional unit g.
$W_v(m)$,$W_q(r)$	Energy limits of hydro unit m and natural gas unit r, respectively.
$V_0(m)$,$V_{\min}(m)$,$V_{\max}(m)$	Initial/minimum/maximum reservoir capacity of hydro unit m.
$I(m, t)$	Cumulative incoming water flow of hydro unit m by period t.
$S(m, t)$	Cumulative surplus water flow of hydro unit m by period t.
$H(m)$	Working head of hydro unit m.
$\eta_v(m)$	Efficiency of hydro unit m.
$\eta_x(c)$	Conversion efficiency of pumped-storage unit c (generally takes 80%).
$\gamma(g, l)$	Power distribution factor of conventional unit g at line l.
$\gamma'(g', l)$	Power distribution factor of RE unit g' at line l.
$P_{L\max}(l)$	Transmission capacity of line l.
$\Delta P_{(1)}(g)$	Allowable power deviation between day-ahead scheduling and first rolling dispatch scheme of conventional unit g.
$\Delta P_{(k)}(g)$	Allowable power deviation between $(k-1)$th rolling dispatch scheme and kth rolling dispatch scheme of conventional unit g.

I. Introduction

INTEGRATION of RE has a great impact on power grid operation and the traditional power grid theories and technologies face challenges. It is internationally recognized that the island (or weak-tie connected) power grids are the best platforms for RE testing and demonstration because of their abundant RE resources, scarcity of conventional energy, and technical difficulty with accommodation of intermittent energy. There have been several successful cases in the world. One famous demonstration of smart grid is the EcoGrid European (EU) project on the Danish Island of Bornholm [1], which aims to contribute to the EU 20-20-20 goals by showing that it is possible to operate a distribution power system with more that 50% renewable energies using smart communication and smart market solutions. There is another case on the Hawaiian Island of Maui [2], which has high RE penetration, advanced adoption of plug-in vehicles, distributed power generation, and isolated island electrical system. The objective is to achieve 40% renewable generation from clean energy by 2030, expanded distributed generation, load reduction, and less reliance on petroleum. Similar demonstrative case can be found on Samsø Island of Denmark, which obtains all of its electricity from wind. Moreover, El Hierro, the most remote one of Spain's Canary Islands will generate nearly all of the island's power from renewable sources by a combination of wind and hydroelectric facilities.

There are also several demonstrative smart grids in China. One of the most important demonstrations lies in Hainan Island, the second largest island in China. The research and demonstration is established on the whole Hainan power grid shown in Fig. 1, which is located at Hainan Island. Various and abundant renewable energies exist on Hainan Island: the onshore wind power capacity to be developed is expected to be 1300 mW; the offshore wind power capacity to be developed is about 5000 mW; the solar power capacity to be developed is about 21 000 mW; and the biomass, tidal energy, and other RE reserves are also very abundant. Currently, the wind power capacity penetration is near to 15%. Hainan power grid is connected to the mainland China Southern power grid using 500 kV submarine cables in 2009, which can assume the contingency reserve not exceeding 600 mW. The normal power exchange is controlled to 0 mW. Hainan power grid is a typical weak-tie (almost isolated) power grid. Research and practice of integration of multitype RE into Hainan power grid has special significance.

Fig. 1. This figure has been deleted due to legal reasons.

TABLE I
Comparison of Island Power Grids Used for Smart Grid Demonstration

Island Name	Bornholm	Maui	Samsø	El Hierro	Hainan
Country	Denmark	USA	Denmark	Spain	China
Area(km^2)	588	1,884	114	276	33,210
Voltage Level(kV)	60	30	NA	15	500/220/35/10
Capacity (MW)	146	119	NA	11.36	3,403
Peak Load (MW)	55	NA	NA	7.56	2,290
Main Generation Resources	wind solar biogas CHP biomass	wind solar coal	wind biomass pumped-storage solar	wind hydro solar diesel pumped-storage	wind hydro solar gas coal pumped-storage nuclear

The comparative data of the above-mentioned demonstrative smart grids are listed in Table I. It is easy to see that Hainan power grid has great advantages not only in scale, but also in types of generation sources and voltage levels. In fact, Hainan power grid is a complete power grid consists of generation,

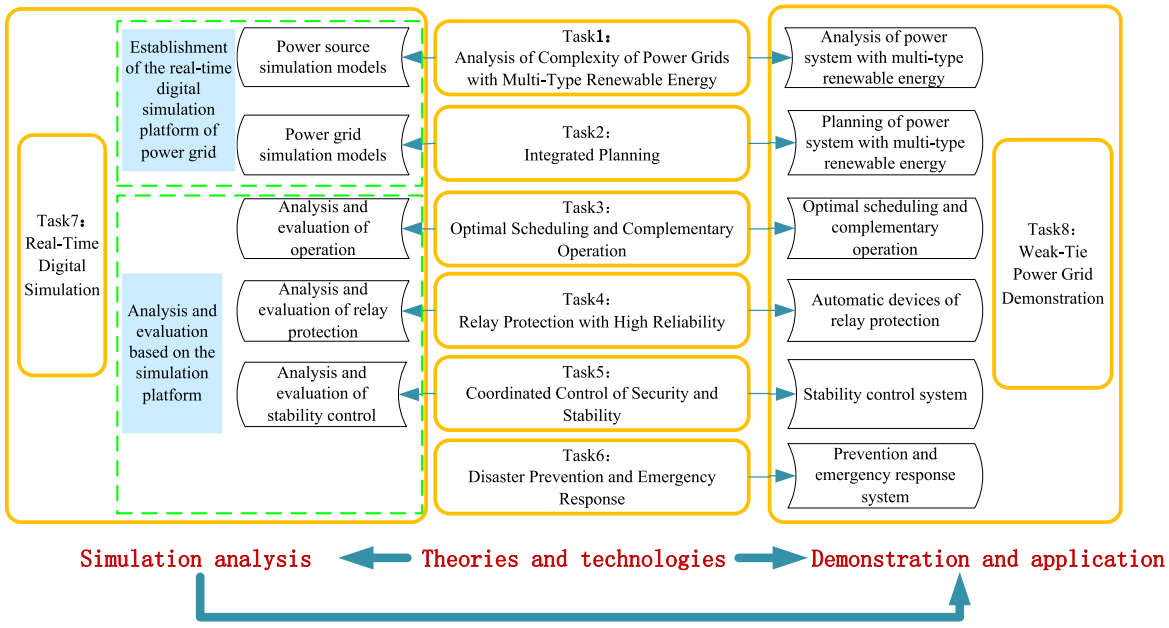

Fig. 2. Architecture of Hainan smart grid research project.

transmission, distribution and demand and appropriately sized for research, other than the distribution networks in most of the other demonstrative cases.

The ongoing research on Hainan power grid will achieve a comprehensive breakthrough in planning, analysis, scheduling, operation, protection, security control, and disaster prevention of power grids with multitype RE integrated. Based on the theoretical research and technological innovation, the country's first demonstrative weak-tie power grid with RE penetration not less than 15% will be established in Hainan. The research consists of three parts as key technology research, simulation platform development, and demonstration and is divided into eight research tasks. The architecture of the project and relationship among the tasks are shown in Fig. 2. A more detailed introduction of the research is referred to [3]. The research will lay a solid foundation for large-scale utilization of RE. For clarity, only the issues on optimal scheduling and complementary operation will be discussed in detail in this paper.

The remainder of this paper is organized as follows. A new framework of multitime-frame robust scheduling/dispatch is proposed in Section II. Then the detailed formulation and solution of robust scheduling/dispatch are given in Section III. Results of the case studies based on the real data of Hainan power grid are reported in Section IV. Finally, Section V concludes this paper.

II. Framework of Multitime-Frame Robust Scheduling/Dispatch

This paper focuses on the topic of robust scheduling/dispatch, which belongs to the third research task—optimal scheduling and complementary operation and is the core of the whole project.

Scheduling and operation of power system with significant wind power penetration are hot research topics at present [4]. Wind power is hard to forecast with great accuracy for dispatching purposes. Hence, there is an unavoidable random error between the actual wind power output and its forecasted value. How to deal with the uncertainty is a difficult issue bringing new challenges to power system scheduling and operation. To accommodate the random wind power fluctuation by reasonable dispatch of the nonwind generation units, one method is to increase the system reserve. However, it is difficult to determine the precise reserve amount which is enough to overcome wind power uncertainty and guarantee system security, and thus the results usually tend to be conservative.

A better alternative is stochastic programming (SP) based on scenarios by which we can obtain more adaptive unit commitment and generation dispatch [5]. Tuohy *et al.* [6] guaranteed that the generation of nonwind units in a predicted scenario could transfer to the responding value in any error scenario within the unit ramping rate limits. In [7], a scenario-based security constrained unit commitment (SCUC) model without reserves was established, considering load forecast errors and system contingencies. Pablo *et al.* [8] further demonstrated that it was the optimal strategy to solve stochastic SCUC when appropriate reserve amount was taken into account. A stochastic method for the hourly scheduling of optimal reserves is presented in [9] when the hourly forecast errors of wind energy and load are considered. The effect of $N-1$ contingencies, wind and load uncertainties, and demand response provider (DRP) bids in the hourly generation scheduling are analyzed. A chance-constrained two-stage (CCTS) stochastic program considering the uncertain wind power output was studied in [10]. The problem is formulated as a CCTS stochastic program. The approaches based on SP are effective for dealing with wind power uncertainties. However, they

are based on wind power probability distribution, which is often difficult to be acquired. Furthermore, they cannot give the clear bound for power system secure operation and also computationally expensive in practical applications.

Currently, there is another trend in research on power system operation planning, which is based on robust optimization (RO). RO was developed to provide a practical approach for handling noisy data and uncertainty [11]. Different from SP, the importance of controlling the variability of the solution (as opposed to just optimizing an expected objective value) is well recognized. The RO framework addresses this issue directly. A RO approach is proposed in [12] to accommodate wind output uncertainty, with the objective of providing a robust unit commitment schedule for the thermal generators in the day-ahead market that minimizes the total cost in the worst wind power output scenario. An innovative minimax regret unit commitment model is introduced in [13], aiming to minimize the maximum regret of the day-ahead decision from the actual realization of the uncertain real-time wind power generation. A RO approach is developed in [14] to derive an optimal unit commitment decision for the reliability unit commitment runs by Independent System Operators (ISOs)/Regional Transmission Organizations (RTOs), with the objective of maximizing total social welfare in the joint worst-case wind power output and demand response scenario. Several U.S. ISOs/RTOs have been working on robust approach to their operational issues, which show its great potentials of practical application. In [15], a framework of using RO-based approach on Midcontinent Independent System Operator (MISO) look-ahead commitment was introduced, with challenges to overcome in order to be practical for real world application. A computational tractable two-stage RO framework for the Pennsylvania-New Jersey-Maryland look-ahead unit commitment with the consideration of load uncertainty is proposed in [16], which can provide sufficient ramping capability and improve the security according to the computational results. ISO New England also reports some results on robust unit commitment and robust economic dispatch [17].

Another related topic is on interval optimization approaches to unit commitment. Wu *et al.* [18] compares applications of scenario-based and interval optimization approaches to stochastic security-constrained unit commitment, and the results show that the interval optimization solution requires less computation and automatically generates lower and upper bounds for the operation cost and generation dispatch, but its optimal solution is very sensitive to the uncertainty interval. A novel unit commitment method based on interval number analysis and optimization was proposed in [19] to accommodate the volatile node injections such as wind power, electric vehicle, and uncertain bus load caused by demand response. Although the interval optimization and RO look rather different, they are similar in expressing uncertainty by a set with a deterministic boundary and avoiding use of probability distribution.

This paper also highlights the idea of power system robust operation, but from a rather different perspective. In existing literature, the engineering characteristics of power system operation (especially different operational strategies in different time frames) have not been sufficiently considered. In essence, the key to robustness is to deal with uncertainty. Robustness of a practical power system would be an integrated solution consists of power forecast, unit commitment, economic dispatch, and control. The main uncertainties of the researched power systems are the power outputs of RE sources, which are caused by inaccurate forecasting. The longer the forecast time horizon is, the bigger the forecast error becomes. As shown in Fig. 3, the wind (solar) power forecast error is much bigger in the day-ahead than in the hours-ahead (intraday) time frame, and with the confidence level of 95%, the confidence interval of day-ahead forecast is much wider than that of intraday forecast. The one-shot robust unit commitment model only makes use of the day-ahead power forecast data and more accurate intraday forecast data are omitted, and then it is hard to provide an optimal strategy in real operation. These errors even sometimes cause disruptions from the day-ahead plan in practical operation. Traditionally, the system operator typically deals with such errors using the intraday and real-time dispatch [20]. This is also the reason for us to adopt a multitime-frame solution—different uncertainties should be handled in different time frames. Based on this consideration, a multitime-frame robust scheduling/dispatch system of power grids with multitype RE is first presented in this paper. The scheduling/dispatch process is shown in Fig. 4.

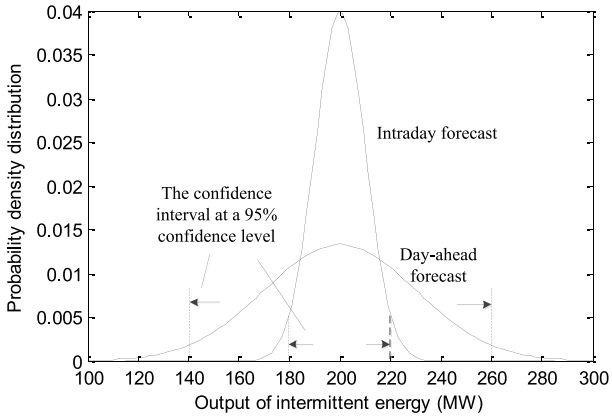

Fig. 3. Probabilistic distribution of day-ahead and intraday intermittent power forecast.

The time frames defined in the robust scheduling/dispatch system are day-ahead, intraday, and real-time horizons. The main functionalities of the three time frames are described as follows.

A. Day-Ahead Scheduling

The unit commitment status and generation levels of all units in the next 24 h will be determined based on day-ahead forecast of load and intermittent power generation. The multiobjective scheduling model should be established if the emissions of pollutants or other objectives are considered. A robust scheduling model based on the concept of extreme scenario is used here to deal with the uncertainty brought by intermittent renewable power generation [4], [21].

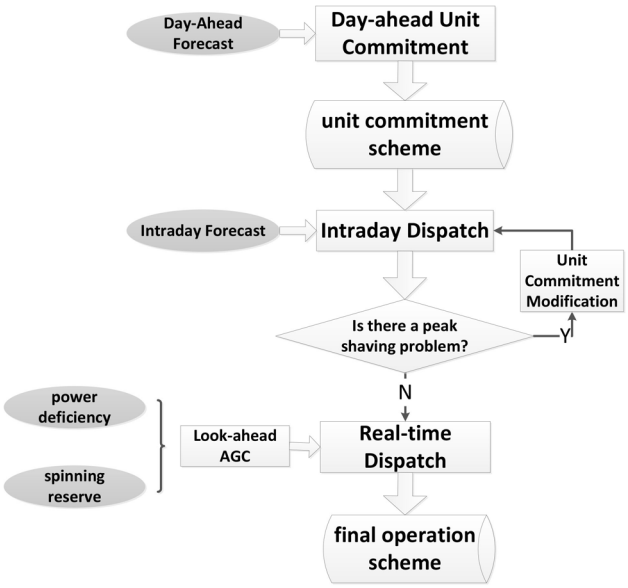

Fig. 4. Framework of multitime-frame robust scheduling/dispatch.

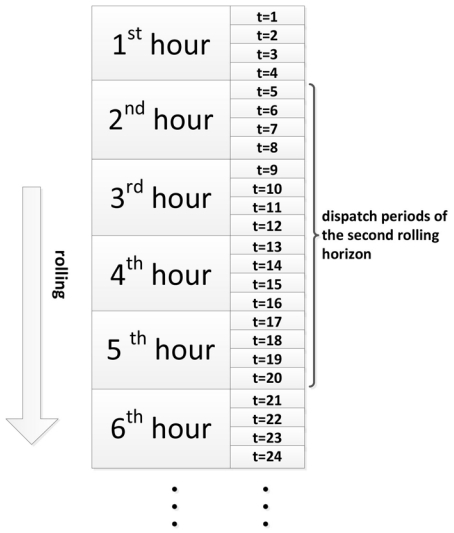

Fig. 5. Illustration of the intraday rolling dispatch.

B. Intraday Dispatch

The intraday rolling dispatch will amend the day-ahead operation plan deviations based on the short-term and ultrashort-term forecast of load and intermittent power generation. In intraday dispatch, if the wind power output deviates significantly from the forecasted value, it may bring peak shaving problem for the system, and the unit commitment should be modified. The strategy used for this intraday rolling dispatch is illustrated in Fig. 5. The rolling dispatch is performed once per hour and the time horizon is four hour. The dispatch time period is 15 min and then there are 16 time periods in a dispatch horizon. As shown in Fig. 5, the first rolling horizon is 1–4 h; the second rolling horizon is 2–5 h, and so on. Each rolling dispatch is performed on basis of the scheme of the last rolling dispatch and the latest ultrashort-term power forecasts. Therefore, the rolling dispatch is a process of continuous revision.

C. Real-Time Dispatch

Real-time dispatch is based on the ultrashort-term power forecast ahead of operation time. The objective of real-time dispatch is to further check and correct the operational plans of other time frames to cope with fluctuations in wind power, loads, and other unpredicted events in real-time. Real-time dispatch not only needs to be coordinated with intraday rolling dispatch, but also need to coordinate with Automatic Generation Control (AGC). A look-ahead control model of AGC that requires real-time estimates of the system's load and intermittent generation is recommended [22].

III. Problem Formulation and Solution

The multitime-frame robust scheduling/dispatch system contains a set of complicated models and algorithms. To make clear, only the day-ahead scheduling and intraday dispatch are discussed here. The results of real-time dispatch are not included.

A. Problem Formulation

A joint dispatch model of coal, hydro, wind, solar, natural gas power plants, nuclear, and pumped-storage is established in this paper.

Suppose there are N coal units, M hydro units, R natural gas units, D nuclear units, C pumped-storage units, J wind farms, and Y photovoltaic plants in a power system, the units except wind and solar power are called conventional units, whose total number is $G = N + M + R + D$. On the other hand, the number of RE unit is $G' = J + Y$. The dispatch horizon is divided into T dispatch periods.

The uncertainty of intermittent power generation can be described by scenarios. In each scenario, the intermittent power generation takes a random value with a certain probability. Three kinds of scenarios are defined here: in predicted scenario, the intermittent power generation takes the predicted value; in error scenario, intermittent power generation is unequal to the predicted value; if the intermittent power generation is equal to the respective confidence limit in a scenario, it is defined as an extreme scenario [4].

The objective function of the dispatch problem can be formulated as

$$\text{Min}: F = \sum_{n=1}^{N}\sum_{t=1}^{T} F_g(n,t) + \sum_{r=1}^{R}\sum_{t=1}^{T} F_q(r,t) + \sum_{d=1}^{D}\sum_{t=1}^{T} F_e(d,t). \tag{1}$$

The objective is to minimize the total generation cost of individual units in the predicted scenario. The hydro, pumped-storage, wind and solar power generation is supposed to have no cost, and then the total cost equals to the cost sum of coal, natural gas, and nuclear power plants. In (1), $F_g(n,t)$, $F_q(r,t)$ and $F_e(d,t)$ are generation cost of coal unit n, natural gas unit r, and nuclear unit d at dispatch period t, respectively. The generation cost are supposed to be the traditional quadratic function of generation output.

The constraints can be divided into three groups: 1) constraints in predicted scenario; 2) constraints in error scenarios; and 3) constraint correlating different scenarios.

1) Constraints in Predicted Scenario:

$$\sum_{n=1}^{N} P_g(n,t) + \sum_{m=1}^{M} P_v(m,t) + \sum_{r=1}^{R} P_q(r,t) + \sum_{d=1}^{D} P_e(d,t) + \sum_{c=1}^{C} P_x(c,t) + \sum_{j=1}^{J} P_w(j,t) + \sum_{y=1}^{Y} P_f(y,t) = P_D(t) \quad (t = 1, 2, \ldots, T) \tag{2}$$

$$P_x(c,t) = P_{x,pm}(c,t) + P_{x,\mathrm{gen}}(c,t) \quad (c = 1, 2, \ldots, C; t = 1, 2, \ldots, T) \tag{3}$$

$$\sum_{g=1}^{G} (P_{\max}(g) - P(g,t)) \geq P_D(t) \times \gamma \ \ (t = 1, 2, \ldots, T) \tag{4}$$

$$P_{\min}(g) \leq P(g,t) \leq P_{\max}(g) \ (g = 1, 2, \ldots, G; t = 1, 2, \ldots, T) \tag{5}$$

$$-R_d(g) \times \tau \leq P(g,t) - P(g,t-1) \leq R_u(g) \times \tau \quad (g = 1, 2, \ldots, G; t = 2, 3, \ldots, T) \tag{6}$$

$$\sum_{t=1}^{T} P_v(m,t) \leq W_v(m) \ \ (m = 1, 2, \ldots, M) \tag{7}$$

$$\sum_{t=1}^{T} P_q(r,t) \leq W_q(r) \ \ (r = 1, 2, \ldots, R) \tag{8}$$

$$V_{\min}(m) \leq V_0(m) + I(m,t) - S(m,t) - Q(m,t) \leq V_{\max}(m) \quad (m = 1, 2, \ldots M; t = 1, 2, \ldots, T) \tag{9}$$

$$P_v(m,t) = 0.00981 \times Q(m,t) \times H(m) \times \eta_{\,v}(m) \quad (m = 1, 2, \ldots M; t = 1, 2, \ldots, T) \tag{10}$$

$$V_{\min}(c) \leq V_0(c) - L(c) \times \Delta P_x(c,t) \leq V_{\max}(c) \quad (c = 1, 2, \ldots C; t = 1, 2, \ldots, T) \tag{11}$$

$$\Delta P_x(c,t) = \sum_{h=1}^{t} P_{x,\mathrm{gen}}(c,h) - \eta_{\,x}(c) \times \sum_{h=1}^{t} P_{x,pm}(c,h) \quad (c = 1, 2, \ldots C; t = 1, 2, \ldots, T) \tag{12}$$

$$\Delta P_x(c,T) = 0 \ (c = 1, 2, \ldots, C) \tag{13}$$

$$\left| \sum_{g=1}^{G} \gamma\ (g,l) P(g,t) + \sum_{g'=1}^{G'} \gamma\,'(g',l) P'(g',t) \right| \leq P_{L\max}(l) \quad (l = 1, 2, \ldots, L; t = 1, 2, \ldots, T). \tag{14}$$

Equation (2) is the power balance equations. Equation (3) is the expressions of pumped-storage units; when unit c is in pumping state, it is regarded as a virtual motor and the power output $P_{x,pm}(c,t) < 0$; when unit c is in generation state, its power output $P_{x,\mathrm{gen}}(c,t) > 0$. Equation (4) is the constraints of spinning reserve. Equation (5) and (6) are generation limits and ramp rate constraints of conventional units. Equations (7) and (8) are energy constraints of hydro and natural gas units, which are converted from the water/gas volume limits. Equation (9) is reservoir capacity constraints of hydropower plants. Equation (10) is the energy conversion equations of hydropower plants. Equation (11) is reservoir capacity constraints of pumped-storage power plants. Equation (12) is the equations of accumulated generation quantity of pumped-storage power plants taking into account both the generation and pumping procedures. Equation (13) requires that the accumulated generation quantity of pumped-storage power plants to be 0 at the end of the dispatch horizon, which means that the reservoir water levels return to the initial values. Equation (14) is the capacity constraints on transmission lines.

2) Constraints in Error Scenarios: Constraints in error scenarios are similar to constraints (2)–(12) in predicted scenarios, except that all generation power outputs should be changed to values in error scenarios. Taking (2) as an example, after we substitute all generation outputs in the predicted scenario to those in error scenario s_i, we can get

$$\sum_{n=1}^{N} P_g(s_i,n,t) + \sum_{m=1}^{M} P_v(s_i,m,t) + \sum_{r=1}^{R} P_q(s_i,r,t) + \sum_{d=1}^{D} P_e(s_i,d,t) + \sum_{c=1}^{C} P_x(s_i,c,t) + \sum_{j=1}^{J} P_w(s_i,j,t) + \sum_{y=1}^{Y} P_f(s_i,y,t) = P_D(t) \ (t = 1, 2, \ldots, T) \tag{15}$$

where $P_g(s_i,n,t)$ is the generation level of coal n at period t in error scenarios s_i, and other notations in (15) have similar meanings. Other constraints can be get in the same way and will be omitted here for limitation of paper length.

3) Constraint Correlating Different Scenarios:

$$-R_d(g) \times \tau_c \leq P\,(g,t) - P(s_i,g,t) \leq R_u(g) \times \tau_c \quad (i = 1, 2, \ldots, Ns; g = 1, 2, \ldots, G; t = 1, 2, \ldots, T) \tag{16}$$

$$-R_d(g) \times \tau_c \leq P(s_i,g,t) - P(s_{i'},g,t) \leq R_u(g) \times \tau_c \times \left(i, i' = 1, 2, \ldots, Ns; g = 1, 2, \ldots, G; t = 1, 2, \ldots, T\right). \tag{17}$$

Equation (16) requires that the operating point of the power system can be readjusted from $P(g,t)$ in the predicted scenario to $P(s_i,g,t)$ in error scenario s_i in τ_c. Equation (17) requires that the operating point of the power system can be readjusted between two arbitrary error scenarios in τ_c.

B. Robust Solution

The security of power system is always of first importance in power system operation. The scheduling/dispatch scheme should meet the requirements of all possible situations (scenarios). However, because the number of scenarios is infinite, we should select some representative scenarios for the calculation. Monte Carlo simulation is used in SP-based approaches for this aim. As a key point of our robust approach, we first introduced the concept of extreme scenario in [4]. Since the concept of extreme scenarios is of special importance, it is further explained as follows.

The scenarios of a wind farm is shown in Fig. 6(a); the scenarios of tow wind farm is shown in Fig. 6(b). Among them, $P_{w,\min}$ and $P_{w,\max}$ are the minimum and maximum possible generation outputs (namely confidence limits) of a wind farm. $S_i (i = 1, 2, 3, 4)$ is the scenario consists of confidence interval

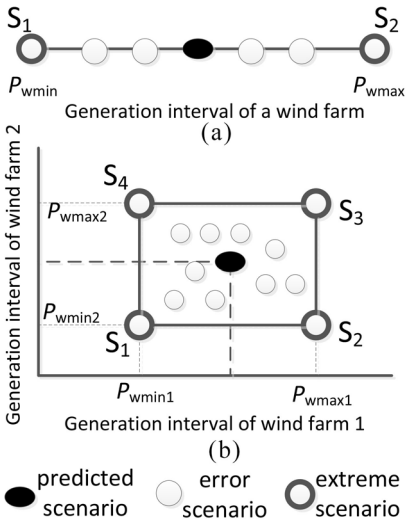

Fig. 6. Definition of scenarios. (a) Scenarios of a wind farm. (b) Scenarios of a tow wind farm.

limits of wind farms, namely the extreme scenario. For a single wind farm, the number of extreme scenarios (S_1, S_2) is 2 and the possible wind generation outputs lie on the line segment between S_1 and S_2. If there are two wind farms, the number of extreme scenarios (S_1, S_2, S_3, S_4) is 4 and the possible wind generation outputs lie in the rectangle made of S_1, S_2, S_3 and S_4. Clearly the value space of wind generation output will be a n-dimensional convex polyhedron with 2^n vertex when there are $n(n \geq 3)$ wind farms.

We have proved in [4] that solution of the model will be robust over all the error scenarios in the value space as long as it is robust over all the extreme scenarios. In the words of RO, the extreme scenarios can be used as the uncertainty set [11]. Then, we can replace all constraints in error scenarios with those in extreme scenarios in the calculation.

C. Model Difference in Different Time Frames

1) Day-Ahead Scheduling Model: Day-ahead scheduling is modeled as robust unit commitment. The robust unit commitment models in [12]–[17] can be adopted. Here the engineering practical model in [4] and [21] based on the concept of extreme scenario is used. The model can be extended on the basis of (1)–(17). The start-up cost should be added to (1) and the variables representing unit commitment status should be included in the constraints (2)–(15). Additional constraints concerning with unit commitment status such as minimum up/down time should be considered too.

The day-ahead scheduling model is a mixed integer programming problem and solved by an optimization solver of CPLEX – 12.1.

2) Intraday Dispatch Model: The rolling dispatch process illustrated in Fig. 5 is implemented as follows.

Because the rolling dispatch is carried out continuously, there is a connection between two successive rolling dispatch processes. The deviation of the first rolling dispatch scheme from the day-ahead scheduling scheme should be limited, and then the deviation of the kth $(k > 1)$ rolling dispatch scheme

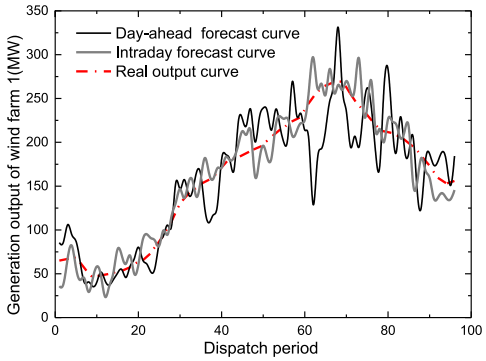

Fig. 7. Real power output, day-ahead forecast and intraday forecast curves of wind farm 1.

from the $k-1$th rolling dispatch scheme should be limited also. The additional constraints can be expressed by

$$\begin{aligned} -\Delta P_{(1)}(g) &\leq P_{(1)}(g,t) - P_{(0)(g,t)} \\ &\leq \Delta P(g)_{(1)} \ (g = 1, 2, \ldots, G; t = 1, 2, \ldots, T) \end{aligned} \tag{18}$$

$$\begin{aligned} -\Delta P_{(k)}(g) &\leq P(g,t)_{(k)} - P(g,t)_{(k-1)} \\ &\leq \Delta P_{(k)}(g) \ (g = 1, 2, \ldots, G; t = 1, 2, \ldots, T). \end{aligned} \tag{19}$$

In the first dispatch period of the kth $(k > 1)$ rolling dispatch, the additional ramp rate constraints should be considered

$$\begin{aligned} -R_d(g) \times \tau &\leq P_{(k)}(g, t = 1) - P_{(k-1)}(g, t = 4) \\ &\leq R_u(g) \times \tau \ (g = 1, 2, \ldots, G). \end{aligned} \tag{20}$$

The intraday dispatch model is a nonlinear programming model and the computation should be carried out online. To increase computational efficiency and consider more engineering characteristics of a real-world power system, the interior point algorithm programmed with C++ is used for solving this model.

IV. Case Studies

A. System Description

The real data of Hainan power grid is used in the simulation. The generation mix is 47.1% coal, 11.4% natural gas, 7.7% hydro, 15.4% nuclear, 3% pumped-storage, 13.2% wind, and 2.5% solar power. There are five wind farms and one photovoltaic plant in this power grid. The wind (solar) power outputs are the main influencing factors of scheduling/dispatch results. Taking wind farm 1 as an example, the forecasting precision in day-ahead and intraday forecast is different as shown in Fig. 3. With the confidence level 95%, the confidence interval of day-ahead forecast is ±30% of the forecasted value, and that of intraday forecast is ±10% of the forecasted value. The curves of real power output, day-ahead forecast, and intraday forecast are shown in Fig. 7. All simulations are performed on a desktop computer with 2.4 GHz CPU and 2 GB RAM.

B. Numerical Results

The unit commitment scheme obtained from day-ahead scheduling is shown in Fig. 8. The solid lines mean

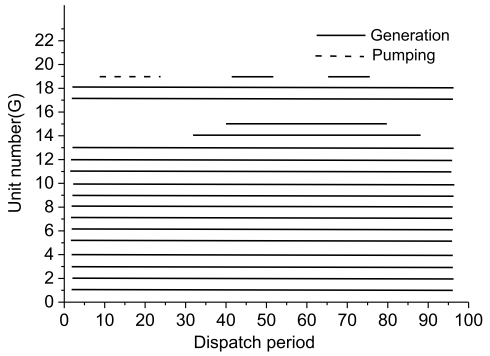

Fig. 8. Day-ahead scheduling scheme.

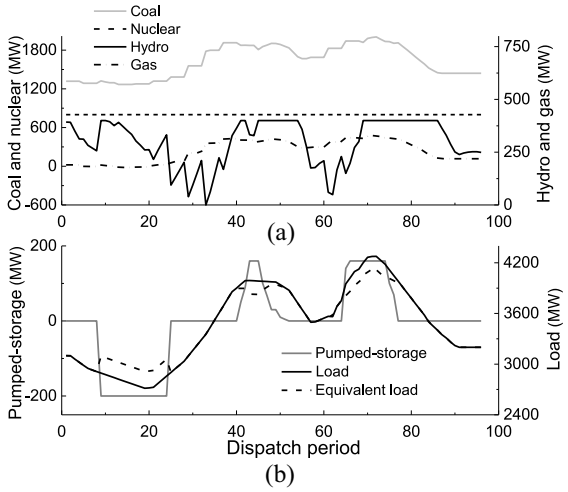

Fig. 9. Intraday dispatch scheme. (a) Generation curves of different types of units. (b) Comparison between the output of pumped-storage units and the load.

that the unit turns on; the dashed line mean that the pumped-storage unit is in the pumping state. Units numbered $1 \sim 9$ are coal units; $10 \sim 12$ are hydro units; $13 \sim 16$ are natural gas units; $17 \sim 18$ are nuclear units; and 19 is pumped-storage units.

The intraday rolling dispatch is calculated based on the unit commitment scheme. The generation curves of different types of units are shown in Fig. 9(a), and the comparison between the output of pumped-storage units and the load is shown in Fig. 9(b). From Fig. 9 we can see the following.

1) Generation curves of nuclear and coal units vary slightly and the frequent adjustment is avoided.
2) Variation of generation curve of natural gas units is consistent with the system load.
3) The hydro units are adjusted frequently to keep power balance of the system.
4) The pumped-storage units generate power at the periods of peak load and pump water at the periods of light load, which shows their function of peak-shaving.

C. Evaluation of Scheduling/Dispatch Schemes

1) Evaluation of Economy and Robustness: Here five scheduling/dispatch schemes are evaluated.

1) Scheme 1 (one time frame) is obtained from traditional day-ahead scheduling, and the spinning reserve for intermittent generation is supposed to be 30% of the forecasted RE generation.
2) Scheme 2 (two time frames) is obtained from traditional intraday dispatch based on the results of scheme 1.
3) Scheme 3 (two time frames) is similar to scheme 2, but the spinning reserve for intermittent generation is supposed to be 60% of the forecasted RE generation.
4) Scheme 4 (one time frame) is obtained from robust day-ahead scheduling.
5) Scheme 5 (two time frames) is obtained from robust intraday dispatch based on the results of scheme 4.

TABLE II
COMPARISON OF FIVE SCHEDULING/DISPATCH SCHEMES

Schemes	Number of time frames	Q_w (MWh)	Q_m (MWh)	F ($)	F_{em} ($)	F' ($)
1	1	8.94	39.77	1124467	130781	1255248
2	2	3.22	17.97	1125273	59026	1184299
3	2	1.36	5.52	1129311	18162	1147473
4	1	0.55	0.32	1131229	1092	1132321
5	2	0	0.23	1127715	752	1128467

Both economy and robustness of the schemes should be evaluated. The extreme scenarios are the worst situations that the scheduling/dispatch schemes can accommodate. When the actual wind power exceeds the confidence limits, emergency measures such as wind power curtailment or load shedding should be adopted. The system power deficiency should be calculated to evaluate possible losses in actual operation. If the power deficiency is positive, the system has excess power and some wind power should be curtailed; oppositely, if the power deficiency is negative, the system has insufficient power and load shedding is needed.

The costs of wind power curtailment and load shedding are introduced to consider the robustness. The cost of wind power curtailment is calculated as $F_w = f_w \times Q_w$, where Q_w is the energy of wind power curtailment and f_w is the cost of wind power per kWh. Because the cost of wind power curtailment can be regarded as an opportunity cost, and that is, when wind power energy Q_w is curtailed, it will be replaced by generation of conventional units, so that f_w can be estimated by the average generation cost of conventional units, and here we assume $f_w = 0.082$ \$/kWh. The cost of load shedding is calculated as $F_m = f_m \times Q_m$, where Q_m is the energy of load shedding and f_m is average outage cost per kWh, and here we assume $f_m = 3.27$ \$/kWh. Then the total cost considering emergency measures can be written as $F' = F + F_w + F_m$, where F is the total generation cost in (1). Here we define $F_{em} = F_w + F_m$ as the emergency cost. The calculation results are listed in Table II.

From Table II, we can see that schemes 1 and 2 have the same spinning reserve, and the generation cost is near. However, because the more accurate intraday forecast is used in intraday rolling dispatch of scheme 2, the robustness is significantly improved (F_{em} is much smaller), which results in a much smaller F'. Both schemes 4 and 5 use robust approaches, which can accommodate random intermittent power fluctuation within the confidence interval and have small F_{em}. Compared with scheme 4, scheme 5 uses two time

TABLE III
POWER FLOW MARGIN OF FIVE SCHEDULING/DISPATCH SCHEMES IN PREDICTED SCENARIO

Scheduling/dispatch schemes	$\delta(l_1,t)$ at peak load period	$\delta_{sum}(l_1)$
Scheme 1	0	12.14
Scheme 3	0	11.39
Scheme 3	0	11.33
Scheme 4	0.23	31.14
Scheme 5	0.07	18.86

frame robust scheduling/dispatch and also takes consideration of day-ahead/intraday intermittent power forecast, and both economy and robustness are improved.

Compared with nonrobust scheme 2, scheme 5 has higher generation cost but much lower emergency cost, and that is, $F_5 > F_2$ and $F'_{em5} < F'_{em2}$, which results in $F'_5 < F'_2$. Although scheme 3 also acquires good robustness by increasing the spinning reserve directly, the appropriate capacity of reserve is not easy to be determined. In fact, the robust scheduling/dispatch approach presented in this paper can be looked as a more accurate way to consider the spinning reserve. Hence scheme 5 outperforms scheme 3 in both economy and robustness, and that is, $F_5 < F_3$ and $F'_5 < F'_3$.

In summary, the two-time-frame robust scheduling/dispatch method reaches the best balance between economy and robustness.

2) Evaluation of Transmission Security: One of the heavy load transmission lines is chosen for security evaluation, which is labeled as l_1. The transmission capacity of l_1 is supposed to be 300 mW. When the intermittent generation outputs equal to their predicted value, the transmission constraints can be satisfied for all five scheduling/dispatch schemes. Here we define a power flow margin index $\delta(l,t)$ to compare the security of different schemes

$$\delta(l,t) = \frac{P_{L\max}(l) - P_L(l,t)}{P_{L\max}(l)} \tag{21}$$

$$\delta_{\text{sum}}(l) = \sum_{t=1}^{T} \delta(l,t). \tag{22}$$

The power flow margin indices of five dispatch schemes in the predicted scenario are listed in Table III. Schemes 1–3 have smaller total power flow margin indices and reach the transmission limit at the peak load period, transmission security cannot be guaranteed when the intermittent generation power varies. Schemes 4 and 5 have appropriate power flow margins and can guarantee transmission security.

Fig. 10 shows the variation of power flow in l_1 when the intermittent power outputs take the real values. For schemes 1–3 shown in Fig. 10(a), power flow in l_1 exceeds its limits at some dispatch periods, which mean that these schemes cannot guarantee transmission security even if there is sufficient spinning reserve. On the other hand, for the robust schemes 4 and 5 shown in Fig. 10(b), power flow in l_1 is always kept within the transmission limits and scheme 5 is more cost-effective.

In summary, traditional scheduling/dispatch has lower generation cost but cannot accommodate the variation of renewable generation output. Robust scheduling/dispatch has higher

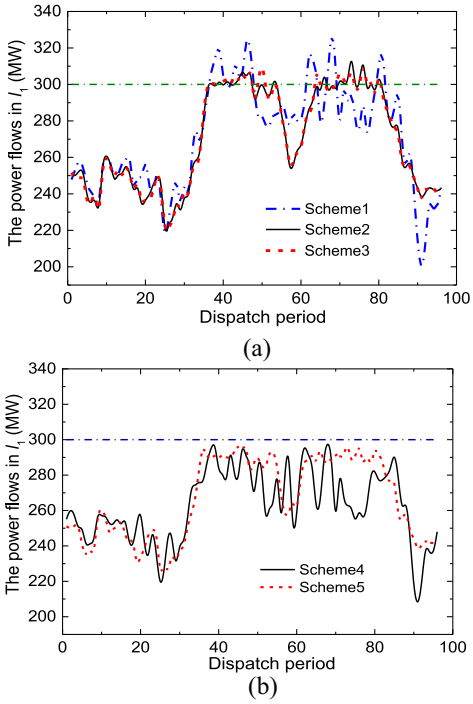

Fig. 10. Power flow in l_1 in five scheduling/dispatch schemes. (a) Schemes 1–3. (b) Schemes 4 and 5.

TABLE IV
PERFORMANCE COMPARISON OF TRADITIONAL DISPATCH AND ROBUST DISPATCH

Dispatch Method	Iterations	Computational time (second)	Generation cost /$	Robustness
Traditional	24	11	high	weak
Robust	29	32	low	strong

generation cost but better robustness, and it also can guarantee security of transmission. The multitime-frame solution is a key to improve economy, robustness, and security.

D. Evaluation of Performance

The day-ahead scheduling is performed once a day, so the computational time requirement is not difficult to be met. The intraday dispatch will be carried out repeatedly and should be finished in a short time, and its computational efficiency is more important. From Table IV, we can see that the computational time of robust dispatch is three times that of traditional dispatch. Because of the advantage of interior point algorithm used, the computational time will not increase exponentially with problem scale. The computational efficiency can be further improved by utilizing sparse technique.

V. CONCLUSION

The ongoing research on Hainan power grid introduced in this paper will achieve a comprehensive breakthrough in power system planning, analysis, scheduling, operation, relay protection, security control, disaster prevention, and other key issues with the multitype RE source integration. This paper focuses on the key part of the research project—optimal

scheduling and complementary operation. The framework of a multitime-frame robust scheduling/dispatch system is first presented and the models and solution methods of day-ahead scheduling and intraday dispatch are given. Computational results based on real data of Hainan power grid show that the robust scheduling/dispatch approach proposed is effective, which reaches a good balance between economy and robustness and will help to deal with uncertainties brought by intermittent renewable sources. The robust scheduling/dispatch framework proposed in this paper is different from most other robust approaches and gives full consideration of the engineering characteristics of power system operation. The scheduling/dispatch system will be put into online operation in the near future.

REFERENCES

[1] J. Kumagai, "The smartest greenest grid," *IEEE Spectr.*, vol. 50, no. 5, pp. 42–47, May 2013.

[2] D. Corbus *et al.,* "All options on the table: Energy systems integration on the Island of Maui," *IEEE Power Energy Mag.,* vol. 11, no. 5, pp. 65–74, Sep./Oct. 2013.

[3] H. Chen, "Key technologies for renewable energy integration—A full scale demonstration at Hainan Island," in *Proc. 5th IEEE PES Asia-Pac. Power Energy Eng. Conf. (APPEEC)*, Hong Kong, Dec. 2013, pp. 1–6.

[4] H. Chen, H. Li, R. Ye, and B. Luo, "Robust scheduling of power system with significant wind power penetration," in *Proc. IEEE Power Energy Soc. Gen. Meeting*, San Diego, CA, USA, 2012, pp. 1–5.

[5] J. H. Wang, M. Shahidehpour, and Z. Y. Li, "Security constrained unit commitment with volatile wind power generation," *IEEE Trans. Power Syst.*, vol. 23, no. 3, pp. 1319–1327, Aug. 2008.

[6] A. Tuohy, P. Meibom, E. Denny, and M. O'Malley, "Unit commitment for systems with significant wind penetration," *IEEE Trans. Power Syst.*, vol. 24, no. 2, pp. 592–601, May 2009.

[7] L. Wu, M. Shahidehpour, and T. Li, "Stochastic security-constrained unit commitment," *IEEE Trans. Power Syst.*, vol. 22, no. 2, pp. 800–811, May 2009.

[8] A. Pablo *et al.,* "Uncertainty management in the unit commitment problem," *IEEE Trans. Power Syst.*, vol. 24, no. 2, pp. 642–651, May 2009.

[9] C. Sahin, M. Shahidehpour, and I. Erkmen, "Allocation of hourly reserve versus demand response for security-constrained scheduling of stochastic wind energy," *IEEE Trans. Sustain. Energy*, vol. 4, no. 1, pp. 219–228, Jan. 2013.

[10] Q. Wang, Y. Guan, and J. Wang, "A chance-constrained two-stage stochastic program for unit commitment with uncertain wind power output," *IEEE Trans. Power Syst.*, vol. 27, no. 1, pp. 206–215, Feb. 2012.

[11] D. Bertsimas, D. B. Brown, and C. Caramanis, "Theory and applications of robust optimization," *SIAM Rev.*, vol. 53, no. 3, pp. 464–501, 2011.

[12] R. Jiang, J. Wang, and Y. Guan, "Robust unit commitment with wind power and pumped storage hydro," *IEEE Trans. Power Syst.*, vol. 27, no. 2, pp. 800–810, May 2012.

[13] R. Jiang, J. Wang, M. Zhang, and Y. Guan, "Two-stage minimax regret unit commitment considering wind power uncertainty," *IEEE Trans. Power Syst.*, vol. 28, no. 3, pp. 2271–2282, Aug. 2013.

[14] C. Zhao, J. Wang, J. P. Watson, and Y. Guan, "Multi-stage robust unit commitment considering wind and demand response uncertainties," *IEEE Trans. Power Syst.*, vol. 28, no. 3, pp. 2708–2717, Aug. 2013.

[15] Y. Chen, Q. Wang, X. Wang, and Y. Guan, "Applying robust optimization to MISO look-ahead commitment," in *Proc. IEEE PES Gen. Meeting*, National Harbor, MD, USA, 2014, pp. 1–5.

[16] Q. Wang, X. Wang, K. Cheung, Y. Guan, and F. S. S. Bresler, "Two-stage robust optimization for PJM look-ahead unit commitment," in *Proc. IEEE PowerTech*, Grenoble, France, Jun. 2013, pp. 1–6.

[17] T. Zheng, J. Zhao, E. Litvinov, and F. Zhao, "Robust optimization and its application to power system operation," in *Proc. CIGRE*, Paris, France, Aug. 2012, pp. 1–8.

[18] L. Wu, M. Shahidehpour, and Z. Li, "Comparison of scenario-based and interval optimization approaches to stochastic SCUC," *IEEE Trans. Power Syst.*, vol. 27, no. 2, pp. 913–921, May 2012.

[19] Y. Wang, Q. Xia, and C. Kang, "Unit commitment with volatile node injections by using interval optimization," *IEEE Trans. Power Syst.*, vol. 26, no. 3, pp. 1705–1713, Aug. 2011.

[20] M. Ahlstrom *et al.*, "Knowledge is power: Efficiently integrating wind energy and wind forecasts," *IEEE Power Energy Mag.*, vol. 11, no. 6, pp. 45–52, Nov./Dec. 2013.

[21] R. Ye, H. Chen, and P. Chen, "Security constrained unit commitment with multiple wind farms integrated," in *Proc. 9th Int. Power Energy Conf. (IPEC)*, Singapore, 2010, pp. 116–121.

[22] D. J. Trudnowski, W. L. McReynolds, and J. M. Johnson, "Real-time very short-term load prediction for power-system automatic generation control," *IEEE Trans. Control Syst. Technol.*, vol. 9, no. 2, pp. 254–260, Mar. 2001.

Haoyong Chen (M'03–SM'10) received the B.S., M.S., and Ph.D. degrees in electrical engineering from Xi'an Jiaotong University, Xi'an, China, in 1995, 1997, and 2000, respectively.

He is currently a Professor with the School of Electric Power, South China University of Technology, Guangzhou, China. His current research interests include power system operation/control, smart grids, computational intelligence applications, and power markets.

Peizheng Xuan received the B.S. degree in electrical engineering from the South China University of Tehnology, Guangzhou, China, in 2013, where he is currently pursuing the M.S. degree.

His current research interests include power system robust dispatch.

Yongchao Wang received the B.S. degree in electrical engineering from Beijing Jiaotong University, Beijing, China, in 2012. He is currently pursuing the Ph.D. degree from the South China University of Technology, Guangzhou, China.

His current research interests include direction is power system optimal operation.

Ke Tan received the B.S. degree in electrical engineering from the South China University of Tehnology, Guangzhou, China, in 2007, where he is currently pursuing the Ph.D. degree.

His current research interests include power system optimal operation and electricity markets.

Xiaoming Jin received the B.S. degree in electrical engineering from the Huazhong University of Science and Tehnology, Wuhan, China, in 1983.

He is currently a Senior Expert with the Electric Power Research Institute of China Southern Power Grid, Guangzhou, China. His current research interests include power system analysis, planning, and operation.

Prof. Jin is a member of the International Council on Large Electric Systems (CIGRE).